Biomimetic hybrid membranes: Incorporation of transport proteins/peptides into polymer supports

Anna Puiggalí-Jou,[1,2,*] Luis J. del Valle,[1,2] and Carlos Alemán[1,2,*]

[1] *Departament d'Enginyeria Química, EEBE, Universitat Politècnica de Catalunya, C/ Eduard Maristany, 10-14, Ed. I2, 08019, Barcelona, Spain*

[2] *Barcelona Research Center for Multiscale Science and Engineering, Universitat Politècnica de Catalunya, C/ Eduard Maristany, 10-14, Ed. C, 08019, Barcelona, Spain*

Correspondence to: anna.puiggali@upc.edu and carlos.aleman@upc.edu

Abstract

Molecular sensing, water purification, and desalination, drug delivery, and DNA sequencing are some striking applications of biomimetic hybrid membranes. These devices take advantage of biomolecules, which have gained excellence on their specificity and efficiency during billions of years, and of artificial materials that load the purified biological molecules and provide technological properties, such as robustness, scalability, and suitable nanofeatures to confine the biomolecules. Recent methodological advances allow a more precise control of polymer membranes that support the biomacromolecules, which are expected to improve the design of the next generation of membranes as well as their applicability. In the first section of this review we explain the biological relevance of membranes, membrane proteins, and the classification used for the latter. Furthermore, the most basic concepts of expression, purification, and refolding of recombinant proteins are briefly discussed. After this, we critically analyse the different approaches employed for the production of highly selective hybrid membranes, focusing on novel materials made of self-assembled block copolymers and nanostructured polymers. Finally, a summary of advantages and disadvantages of the different methodologies is presented and the main characteristics of biomimetic hybrid membranes are highlighted.

Introduction

An ambitious goal of today's synthetic biology, nanotechnology, and bioengineering, is to build constructs analogous to natural systems for tuning and manipulating their complex physical and biological properties. Within this framework, protein-based nanomaterials offer countless potential for biophysical and nanobiomedical applications and serve as new tools for investigating essential biological questions.

Particularly, membrane proteins (MPs) are important key regulators in many biological processes, such as ion transportation, generation of energy and transduction of signals across cell membranes.[1] Besides, MPs constitute about one third of all protein coding genes and are the targets of a huge amount of pharmacological agents.[2,3] Although knowledge about their structure and function is crucial for the proper interpretation of numerous biologically relevant phenomena, these investigations are often very difficult due to the great complexity of cell membranes. Therefore, there is a continuously growing interest in the development of model systems able to offer suitable platforms to address the above mentioned issues. The most popular models include proteoliposomes, lipid monolayers, and solid/supported lipid bilayers. Beyond the use of natural products, it is also possible to incorporate MPs into artificial materials, such as synthetic polymers, which can provide new properties (*e.g.* easiness of handling, robustness, and functionalization). Thus, the biological molecules can bring specificity and efficiency, while the robustness and the possibility of tailoring materials to improve the final functionality can be added by the synthetic polymer. As a result, a wide range of applications have been investigated, including, DNA sequencing,[4] drug delivery,[5] sensors,[6] water desalination,[7,8]and bioelectronics.[9]

Although in the last decade some general reviews on biomimetic membranes have been reported,[1,10–13] in this work we offer a new perspective. More specifically, in this

review we discuss recent developments and advancements from a processing point of view. Thus, the classification of the different approaches used to incorporate MPs onto artificial polymeric supports has been our primary focus, also giving special emphasis to the analysis of the achieved applications.

Membrane proteins (MPs)

The structure of biological membranes is mainly driven by the lipid bilayer, even though the majority of its particular functions are played by the proteins embedded in it.

Lipid bilayers allow facile and rapid diffusion of small non polar molecules such as O_2 (2.3×10^{1} cm/s)[14] and CO_2 (3.7×10^{-1} cm/s),[15] and slower diffusion of small polar but not charged molecules like H_2O (3.7×10^{-3} cm/s),[16] urea and glycerol (~10^{-6} cm/s).[17] On the other hand, biological membranes are reluctant to allow the diffusion of charged molecules (ions) no mattering how small they are, because of the charge and their elevated hydration level. For example, the permeability coefficient of Na^+ and K^+ is ~10^{-14} cm/s.[18]

Although lipids constitute a great part of the membrane biological cells, the high efficiency of the latter for selectively transporting materials across the bilayers is due the presence of MPs.

The numbers in the protein data bank (PDB) reveal that, in comparison with soluble proteins, the quantity of MPs structures analysed is much lower. This feature can reflect the extra difficulties related to the purification and refolding process of MPs.[19] The proteins of interest can rarely be purified from its original membrane because usually their concentrations are not enough.[20] For that reason, MPs need to be overexpressed, which is performed in different host cells, purified, and refolded.

The proteins that are currently attracting considerable interest for preparing hybrid membranes due to their functions and easy overproduction are:

- Water channel MPs, known as aquaporins (Aq), are very attractive because of their high water transport rate and selectivity that can be used for water purification and desalination. The structure of Aq monomers consists in six transmembrane helices and two short helical segments (Figure 1a), which surround the cytoplasmic and extracellular regions, connected by a narrow aqueous pore.[21] When located in the lipid membranes, Aq monomers associate into tetramers, each monomer functioning independently. Nevertheless, a few unsolved questions still remain: is the protein capable to withstand certain conditions (*e.g.* high salinity pressure)? and how can be increased the size of the membranes without any rupturing? In the last five-six years, this field of study has increased considerably.[22-30]

- α-hemolysin (α-HL) is a protein found in the human pathogen *Staphylococcus aureus* bacterium, which is secreted by most strains and acts as a toxin producing haemolysis. However, in the field of nanotechnology, recently, has been reported as useful component for sensors since it allows the facile translocation of single stranded DNA unravelling its coiled structure. When molecules pass through the nanopore they block it reducing the ionic current and each nucleotide provokes a particular reduction.[31,32] This porin is very stable and its functionality prevails at temperatures close to 100 ºC.[33] Because the interior diameter is similar to the diameter of a single nucleic acid strand, the current of ions through the nanopore is partially blocked when the translocation occurs (Figure 1b). More specifically, as each nucleotide produces a different reduction in the ionic current,[34] the

incorporation of α-HL to artificial polymer membranes could be employed to detect DNA sequences through this signal.[35]

- Gramicidin (gA), a hydrophobic pentadecapeptide with a length of 22 Å (Figure 1c),[36-38] organizes in an ion channel that is specific for monovalent cations. This biomolecule has been extensively used as model to study the organization and function of channels-containing membranes.[38]

- Outer membrane proteins (OMPs) are typically employed for the fabrication of hybrid biomimetic membranes. The outer membrane is a protecting barrier of gram-negative bacteria. Unlike the MPs located at other systems, the structure of OMPs does not contain α-helices but instead anti-parallel β-barrels (Figure 1d).[39] OMPs allow the unspecific passive diffusion of ions and molecules across the membrane. The driving-force is the concentration gradient, whereas the limitation lies on the molecular size since the diffused specie needs to be smaller than the pore.

Incorporation onto polymeric substrates

Within the field of biomimetic membranes there is a wide range of strategies and materials studied until now. The modification of artificial membranes with functional molecules within their pores or onto their surfaces, as well as the preparation of artificial channels embedded into block copolymers or lipid bilayers, have already been extensively reviewed by other researches.[10] Here, we focus on the group that involves the complete incorporation of proteins into hybrid polymeric systems. Thus, our main objective is to illustrate the synthetic processes and the materials used for the development of biomimetic hybrid membranes. Table 1 summarizes the different approaches employed until now that, from the perspective of the employed materials,

has been categorized as those based on the utilization of amphiphilic copolymers and nanostructured polymers.

Amphiphilic copolymers

This is the most extensive kind of material employed for manufacturing biomimetic hybrid membranes. Amphiphilic block copolymers can act as artificial building blocks for the generation of membranes capable of incorporating proteins, as do the lipid bilayers. However, the former present other important advantages, such as long-term mechanical stability, tailorable structural parameters and versatile chemical functionality. In dilute aqueous solution, they self-assemble by hydrophobic driving forces, forming different of morphologies, such as spheres, cylinders or lamellas.[40] Amphiphilic copolymers are mostly prepared as diblock copolymers with one hydrophobic and one hydrophilic block or as triblock copolymers with two hydrophilic blocks separated by one hydrophobic, the latter being usually named ABA block copolymers. Despite membranes made of amphiphilic copolymers present high mechanical and chemical stability, low water and gas permeability, and customizable properties (*e.g.* a wide range of membrane thickness), they exhibit some drawbacks with regard to lipid membranes: lower dynamics/fluidity of the bilayer, higher thickness, and lower flexibility. Overall, amphiphilic copolymers hold great potential over lipids as building blocks.[35,41-45]

A large variety of amphiphilic copolymers have been designed using different monomers and applying diverse synthetic techniques,[45] such as anionic[46] and cationic polymerizations,[47] controlled radical polymerization,[48,49] ring-opening polymerization,[50] and "click" chemistry.[51,52] Furthermore, advanced individual properties can be added to the building blocks, as for example the regulation of hydrophilicity and hydrophobicity

of the blocks, block lengths and length ratios, the functionalization of polymer block,[53] the addition of stimuli-responsive polymer blocks,[54,55] and the use of biodegradable polymers.[56] Two of the most interesting modifications reported in the literature are based on the addition of: (*i*) methacrylate units to stabilize the membrane by cross-linking;[57] and (*ii*) dyes for imaging.[58]

In order to mimic cell membranes, block copolymers can be used without any support (free-standing or self-supported), spread and non-covalently or covalently tethered onto solid supports, spread onto porous solid supports, and bounded as polymer vesicles onto a 2D surface.

Free-standing block copolymers

One of the most straightforward methodologies to study the transport across a membrane is having it as separator of two media and to investigate the exchange of solutes and ions concentrations between them. The experimental set-up required for such studies typically includes free-standing membranes. Although a huge amount of studies have been reported, these are mainly based on free-standing lipid bilayers while only a few of them involve block copolymer. This has been attributed to their lower lateral tension, which could lead to a rapid membrane rupture.[59] In an early study, artificial and stable giant free-standing monomolecular films of functionalized poly(2-methyloxazoline)-block-poly(dimethylsiloxane)-block-poly(2-methyloxazoline) triblock copolymer, named PMOXA−PDMS−PMOXA, were prepared for the first time.[43] These copolymer films, which exhibited areas of up to about 1 mm^2 and thickness of 10 nm, were post-polymerized by UV light using the methacrylate groups found at both chain ends. The reconstitution of a porin in the preformed layer was achieved by adding a certain amount of the protein to each side of the chamber and, in particular, the

incorporation was favoured by applying a potential of 20 mV across the membrane. Despite the high thickness of the polymer membrane compared to lipid ones, the protein was successfully incorporated, leading to an enhancement of the conductance across the layer.[60]

More recently, Wong *et al.*[61] used PMOXA−PDMS−PMOXA copolymers to compare the voltage gating ability and threshold voltages of OmpG and alamethicin embedded in lipid bilayers and polymer membranes, which were used to separate two solutions. The molecular properties of the protein (*i.e.* conductance, voltage gating and mobility) were similar for polymer- and lipid-based systems.[61] Ho *et al*.[62] studied the effect of the length of PMOXA−PDMS−PMOXA on protein insertion at the air/water interface. Wilhelmy surface pressure measurements (mN/m) revealed greater OmpF insertion for shorter copolymer chains, which was attributed to their enhanced biomimicry of natural lipid-based membranes.[62]

Block copolymers immobilized onto solid supports

Obviously, the use of solid supports for membrane immobilization provides mechanical stability at the air/water interface and even in the dry state monolayers and or free-standing membranes.[63] The easiest procedure to obtain synthetic solid-supported membranes is the fusion and spreading of polymersomes onto the support (*i.e.* gold or glass surfaces). Moreover, in order to attain stronger fixation it is interesting to promote the chemical bond formation between reactive groups on the surface and reactive end groups of the polymer, or by physisorption of block copolymers with 'sticky' segments.[64] Furthermore, increasing functional group density on the substrate could lead to high area coverage.

Dorn *et al.*[65] formed polymersomes with poly(butadiene)-*b*-poly(ethylene oxide), PB-PEO, which were subsequently spread into glass and gold substrates. For the chemical immobilization onto the gold surface, PB-PEO was functionalized with sulfur-containing lipoic acid (LA), which binds properly to the gold surface (Figure 2a). Covalently bound layers were further incubated with polymyxin B, a peptide able to disrupt lipid membranes.[66] The, resistance of the membranes without and with the peptide, as determined by electrochemical impedance spectroscopy (EIS), was 4.4 and 1.2 $M\Omega \cdot cm^2$, respectively, evidencing that the peptide was successfully embedded. Nevertheless, after 7 hours the resistance increased again due to the loss of peptide.[67]

In comparison to the previous example, Zhang *et al.* [35] combined two methodologies to obtain a defect-free layer onto a gold substrate. More specifically, Langmuir-Blodgett (LB) and Langmuir-Schaefer (LS) deposition techniques were applied using different terminated polymers: LA functionalized linear PB-PEO (PB-PEO-LA) and hydroxyl-functionalized linear PB-PEO (PB-PEO-OH), respectively (Figure 2b). Both techniques enabled a strict control of the layer density by regulating the surface pressure of the molecular assembly. Moreover, combination of both methods led to the achievement of large-area, homogeneous, defect-free layers, which were closer to cell membranes. Again, the protein was added after the layer formation and was monitored by measuring the conductance through the PB-PEO layer before and after the addition of α-haemolysin (αHL), at a voltage of 40 mV. A significant increase in conductance was observed after 20 min of the protein addition.

The same two-step methodology was employed by Kowal *et al.*[67] to generate defect-free layers on solid supports. In this case the PDMS-*b*-PMOXA di-block copolymer with aldehyde ending groups was used to promote the covalent attachment of the polymer membrane through formation of an imine bond with an amino modified gold

substrate. More specifically, such authors studied the effectiveness of bio-beads (BBs) (*i.e.* non-polar polystyrene adsorbent material) as facilitators of protein incorporation (Figure 3a). Their high surface adsorbing area for organic molecules with a MW lower than 2000 KDa allows the proper removal of the detergent used for protein solubilization, thus promoting the incorporation of the protein onto the polymeric bilayer due to its hydrophobicity. Changes in the conductance of gold substrates were recorded to examine the effects associated with the attachment of the polymer layer and the incorporation of protein and bio-beads. Results showed an increase in the substrate conductance when the protein was incubated with bio-beads, whereas no significant increase was found when the protein was incubated without bio-beads, demonstrating that the latter are necessary to incorporate the protein (Figure 3b). Thus, bio-beads act as driving force for the insertion of MPs into polymer membranes attached to solid substrates.

Block copolymers suspended onto porous solid supports

Due to the low stability and difficulty of handling of free-standing copolymer membranes and to the limitations presented by solid supported layers, the field evolved towards copolymer films suspended onto porous solid membranes. In this approach, some zones of the membrane are still free-standing, allowing molecular diffusion without any disturbance.

In a pioneering study, Gonzalez-Pérez *et al.*[68] obtained stable triblock copolymer membranes using scaffolds containing 64 apertures of 300 μm diameter each. The membranes showed high stability, which was evidenced by a long life-time when high polymer concentrations were used (*i.e.* it was stable several days). In order to

incorporate ion channels, GA was reconstituted on these membranes and assembled into dimeric channels.

More recently, Wang *et al.*[22] presented a new strategy to produce planar pore-spanning biomimetic membranes using proteopolymersomes made of PMOXA−PDMS−PMOXA and Aquaporin Z (AqpZ) (Figure 4a). Poly(carbonate) tracked-etched (PCTE) membranes with average pore sizes of 50, 100 or 400 nm were modified with a thin gold layer (60 nm thickness). Then, cysteamine was deposited through chemisorption over the gold surface and the amine residues were transformed into acrylate residues via conjugation of acrylic acid (Figure 4b). Proteopolymersomes were spanned over the surface (Figure 4c) and by covalent-conjugation-driven the vesicle rupture occurred (Figure 4d). Although all the substrates were covered by adapting the pressure to the pore size, membranes with 50 nm pores had much fewer defects compared to the supports with bigger pores.

Duong *et al.*[27] spanned polymersomes over porous alumina substrates of different pore diameters, 55 and 100 nm, covered with gold. Substrates with pores of 100 nm resulted uncovered by the membrane film because the spacing was too large, which supported the findings of Wang *et al.*[22] However, authors successfully deposited AqpZ-containing proteopolymersomes onto the alumina with pores of 55 nm, preserving the natural functionality of the protein (Figure 54).

Following this approach but using new materials, planar biomimetic membranes consisting of AqpZ embedded into PMOXA−PDMS−PMOXA layers were fabricated upon a cellulose acetate (CA) substrate functionalized with methacrylate end groups.[69] Proteopolymersomes were spanned over the CA surface and photocross-linked using UV radiation. The resulting bioinspired device consisted on a selective layer upon the substrate for nano-filtration (Figure 6). Although this technique presents advantages

over the previous ones, it still shows many limitations, such as poor area coverage, membrane defects and difficult scalability to support industrial applications. A similar but at the same time different strategy consists of depositing undisrupted proteopolymerosomes onto porous substrate. Hence, solutes need to cross the whole vesicle and then go through the substrate pore.

Wang *et al.*[29] constructed a new design based on a PCTE membrane (pore size 50 nm, porosity 20%) coated with a 50 nm gold layer by vapour deposition. Then, UV cross-linked vesicles were dropped onto the PCTE surface under vacuum. This allowed exerting certain pressure, facilitating the intrusion of the vesicles. The bare gold surface, which was not occupied with protein containing polymersomes, was further functionalized with a self-assembled monolayer of cysteamine. Later on, vesicles were immobilized on the membrane through an optimized layer-by-layer polydopamine (PDA)–histidine (His) coating process (Figure 7).

A similar methodology but using CA with an average pore size of approximately 25 nm as solid support was reported by Xie *et al.*[30] The UV-crosslinked Aqpz-polymer vesicles were covalently immobilized onto the CA membrane through an amidation reaction between the amino groups on the CA membrane surface and the carboxyl groups on the vesicle surface. Finally, a dense hydrophobic polymer layer was generated by in situ "surface imprinting" polymerization (Figure 8). This innovative membrane, which presented pores smaller than perforated PCTE,[29] exhibited good and controlled selectivity together with high mechanical strength and stability during the nanofiltration.

Proteopolymersomes covalently bounded to a solid support

The last methodology reviewed in this section is the covalent attachment of proteopolymersomes onto a solid surface, which has also been previously employed for lipids.[70] In order to obtain nanoreactors that could carry out conversions at a precise location for the sensors development, Grzelakowski *et al.* [58] applied this approach using block copolymers. For this purpose, an acid phosphatase was encapsulated and the intrusion of the substrate inside the vesicle was provided by the reconstitution of OmpF onto the polymersome membrane. The resulting proteopolymersomes were immobilized into the substrate (*i.e.* glass) by employing the receptor–ligand pair, biotin–streptavidin.[71] The de-phosphorylation of the fluorogenic substrate ELF^{TM} 97 by acid phosphatase was monitored. It was observed that the reaction did not occur when OmpF was not reconstituted, confirming the importance of the protein for the diffusion of certain molecules across the membrane.

More recently, Zhang *et al.*[72] developed "active surfaces" for selective biosensing of sugar alcohols with time and space precision (Figure 9). This bioactive platform was based on the immobilization of nanoreactors with specific MPs inserted in their membranes and sugar alcohol sensitive enzymes encapsulated in their cavities. Interestingly, the artificial surrounding within such a copolymer membrane and the high membrane thickness did not affect the functionality of the reconstituted glycerol facilitator (GlpF), which allowed the selective flux of sugar alcohols into the inner cavity of the polymer nanoreactors where the encapsulated enzymes acted as biosensing entities. An advantage of encapsulating the enzymes inside polymersomes was their protection from a potentially harmful environment, while retaining their catalytic activity. Thus, this smart approach prolonged the life-time of the enzymatic biosensor. The selective permeability of such interesting protein-polymer nanoreactors offers the

opportunity of monitoring the concentration of biologically relevant sugar alcohols since GlpF is able to conduct other sugar alcohols.

Nanostructured polymers

Researchers have focused on amphiphilic polymers for mimicking biological membranes. However, an inconvenient of amphiphilic polymer membranes is that, although the system turns out to be more stable than biological membranes, it is not strong enough to endure many practical applications.[73] In this section we discuss the use of confined biological ion channels prepared by incorporating proteins into pores of nanostructured polymers. A common methodology to control the pore size is the track-etch technique.[74] More specifically, polymer membranes are perforated when heavy ions go through the film and create damage zones on the latent track. Then, these can be converted into a pore by employing the right solution. The size and shape of the pore are regulated by varying the chemical etching conditions (*e.g.* time, temperature and solution concentration).

Balme et al.[73,75] developed hybrid nanoporous membranes handling commercial track-etched poly(carbonate) (PC) films of 5 μm thickness covered with poly(vinylpyrrolidone) (PVP). The resulting nanopores, which exhibited a diameter of 15 nm, were filled with gA. Protein confinement was facilitated by the hydrophobicity of the inner parts of the membrane. Later on, the ion flux passing through the resulting hybrid membrane was evaluated by placing it between two compartments filled with a given electrolyte and pure water, respectively. Although results about the selectivity of the protein were unclear, ion diffusion was significantly higher when the protein was loaded inside the nanopores of the membrane.

The effect of the pore size was studied in a more complex system in which nanostructured polymer membranes were obtained by track etching poly(ethyleneterephthalate) (PET) films. This was followed by the deposition of a multilayer of aluminium oxide/zinc oxide to decrease the initial diameter of the pores from 36 nm to 10.6, 5.7 and 2 nm on demand (Figure 10).[80] Results evidenced that the relative contribution of the ion transport through gA increases with decreasing pore diameter. However, this effect was accompanied by a loss of specificity due to the disassembling of the head-head dimer structure.

Within this context, an interesting OMP, named Omp2a,[77-79] was embedded in a supported poly(*N*-methylpyrrole) (PNMPy) membrane.[80] Figure 11a illustrates how the incorporation of the protein caused significant changes in the surface morphology of PNMPy. Thus, scanning electron microscopy (SEM) micrographs of PNMPy−Omp2a present elements of both submicrometric and micrometric dimensions with a very homogeneous and smooth texture, whereas the nodular outcrops typically found in PNMPy films (Figure 11b) are not detected. These features, which reflected the presence of the protein, were correlated with EIS measurements. It was observed that Omp2a promotes preferentially the passive transport of K^+ with respect to Na^+ in solutions with relatively high ionic concentrations. Nevertheless, PNMPy membrane was electrochemically synthesized onto the electrode (*i.e.* stainless steel), which represented a disadvantage for possible future applications because the membrane cannot be detached from the electrode due to its high fragility.

More recently, instead of using conducting polymers as support for the protein, nanoperforated biodegradable poly(lactic acid) (PLA) nanomembranes were used.[81] These membranes, which were self-standing, were prepared by spin-coating a mixture of poly(vinyl alcohol) (PVA) and PLA, which are immiscible polymers.

Nanoperforations with diameter of 51±22 nm resulted from the combination of nanophase segregation processes and selective solvent etching (Figure 11c).[82] In order to confine the protein into the nanopores, these membranes were incubated in protein solutions and, subsequently, washed many times. Contrast 3D AFM height images painted with phase skin surfaces of samples before and after incubation confirmed the presence of adsorbed oval protein aggregates around and inside the nanopores (Figure 11d). Specifically, phase channel allowed to differentiate Omp2a domains (*i.e.* dark purple aggregates with an average diameter 27 ± 5 nm) from the PLA substrate (coloured in green) where they are adsorbed onto. Moreover, EIS assays showed an increase of conductivity and selectivity against some ions when the protein was confined onto the nanopores.[81]

The thermomechanical properties of this OMP had also been characterized by immobilizing it on microcantilevers.[83] It was found that heat promotes local orientation of the immobilized biomolecules. Thus, appropriate thermal treatments could be employed to enhance the selective ion transport of the substrate since more proteins would be correctly oriented with the required thermal treatment. More interestingly, its functionality onto lipid bilayers, which represents an environment closer to the one on its biological conditions, had also been characterized.[84] The resistance of 40 w/w lipid-to-protein ratio supported lipid bilayers (1.5 kΩ cm^2) was found to be similar to that of nanoperforated Omp2a-filled PLA membranes[81] (1.9 kΩ cm^2) and higher than that of PPy-Omp2a[80] (243 Ω cm^2). As it was expected, the resistance of all systems decreased when the protein was incorporated, this effect being more pronounced for KCl electrolytic solutions. Besides, the resistance variation and the selective ion diffusion unambiguously evidenced the successful incorporation of bioactive porin.

Recent applications of hybrid membranes

Water purification is the greatest and most advanced field for biomimetic membranes, being AqpZ the broadest investigated protein for such function due to its high stability, large water permeability and selectivity. However, the use of amphiphilic bilayers can obscure its selectivity because of the macroscopic defects within the layers producing low salt rejections between 20 and 60%.[85] Ongoing membranes consist on thin-film composite made of polyamide with a salt rejection of 99.85% salt and with water permeability of 1-3 L m^{-2} h^{-1} bar^{-1} (LMH/bar) in reverse osmosis. If we compare these values to the hybrid membranes described in this review, used in forward osmosis it is possible to observe that they have higher water flux (from 5.5 to 17.6 LMH or 8 to 34 LMH/bar) but less salt rejection (from 34 to 98.8 %).[22,69,27,29,30] Therefore, there is still space for improvements. Of utmost relevance is to attain higher rejection of boron and chloride reducing the number of times that actual membranes need to be used. More demanding is the upgrade to hydrophobic molecules rejection. These include many organic micropollutants which can rapidly go through the biomimetic layer. In order to overcome this issue Werber *et al.* proposed to form biomimetic selective layers on top of the typical employed membrane for reversed osmosis. [86] Therefore, this composite would benefit from the advantages of each component leading to membranes with acute ion rejection without losing the removal of hydrophobic neutral micropollutants. One pending issue about the newly generated biomimetic membranes is their long term performance, stability and reusability.

Another new and original application to harvest solar energy for direct electrical power, sensing, or chemical production is the use photosynthetic proteins. [87] Photosystem I has been immobilized in a layer composed of poly(butadiene)$_{12}$-

poly(ethylene oxide)$_8$ (PB_{12}-PEO_8). In order to connect these membranes with the electrodes, conjugated oligoelectrolytes were intercalated within the PB_{12}-PEO_8 layer.

Single molecule detection also offers a great potential because of the channels intrinsic characteristics. Since when a molecule is translocated disturbs the ionic current through the channels leads to unique fingerprint for facile detection.

Conclusions and outlook

Biological membranes are complex systems with many molecules playing crucial interactions, which allow the communication between different compartments or directly permit cell-cell contacts. The study of these events is complicated and, therefore, artificial model membranes play an important role for unravelling the chemical and physical characteristics of the embedded proteins together with their functionality.

In early studies, phospholipid bilayers deposited onto solid substrates (so-called solid-supported membranes) were commonly used as experimental cell-surface models to gain insight into immune reactions and cell adhesion.[88-95] Eventually, mimicking properties of biological elements to prepare functional hybrid materials based on polymers started to be an attractive alternative to the use of lipid bilayers. Polymer membranes in a variety of conditions (*i.e.* free standing films, solid-supported membranes, membranes spanned over porous supports, and proteopolymersomes embedded onto porous substrates) were used to insert membrane proteins not only for understanding their biofunctionality in synthetic templates but also for developing active surfaces for translational applications, such as water purification, molecules biosensing, DNA sequencing, and ion transport.

Within this context, block copolymers have been frequently used to prepare the bilayers supported on a material surface. Such block copolymer-based supramolecular assemblies exhibit many interesting properties, as for example stability, robustness, and tunability. However, many of the proteins employed for basic biophysical studies or for sensor applications are known to protrude from the bilayer. These protruded parts may form strong interactions with the substrate, leading to a partial loss of functionality or even to a complete denaturation.[96] For that reason, different attempts have been done to maintain the distance between the substrate and the proteins, such as the use of nanoperforations to suspended bilayers, the addition of polymer cushions, or the study of proteopolymersomes covalently linked to a solid support. A summary of the advantages and drawbacks of each system is depicted in Table 2.

The approach based on the confinement of the protein on nanostructured polymers is particularly interesting. Polymeric membranes with nanopores and nanoperforation can be prepared by track-etching and by phase segregation, the latter offering better outlook for practical use. However, huge challenges still lie ahead both in terms of "on demand" inducing properties whilst the architecture of the membrane is preserved and of multi-functionality, which can be reached by inserting different MPs or by inserting the MPs at specific locations.

It is worth to mention that in terms of applicability, it is difficult to scale-up the production of these membranes because above all the production and folding of ion-channels is time consuming and expensive. However, over more than three decades the production of synthetic ion channels has been growing. Nowadays, there are many approaches based on chemical synthesis and supramolecular assembly to biomimick macromolecules.[97,98] For example, chloride selective channels had been prepared via directional assembly of electron-deficient iodine atoms, which create a transmembrane

pathway for facilitating anion transport,[99] potassium ion channels by means of aromatic stacking of helical oligomers,[100] or even artificial channels sensible to an external stimuli.[101]

Overall, the integration of biological and synthetic materials is still a promising area of research that awaits further developments. There are many different proteins with useful and accurate functions that upon incorporation on stable polymer membranes could proportionate many unique and beneficial applications.

Acknowledgements

Authors acknowledge MINECO/FEDER (MAT2015-69367-R) and the Agència de Gestió d'Ajuts Universitaris i de Recerca (2017SGR359). Support for the research of C.A. was received through the prize "ICREA Academia" for excellence in research funded by the Generalitat de Catalunya.

References

1 S. Demarche, K. Sugihara, T. Zambelli, L. Tiefenauer and J. Vörös, *Analyst*, 2011, **136**, 1077.

2 E. Wallin and G. Von Heijne, *Protein Sci.*, 2008, **7**, 1029–1038.

3 M. C. Fiori, Y. Jiang, W. Zheng, M. Anzaldua, M. J. Borgnia, G. a. Altenberg and H. Liang, *Sci. Rep.*, 2017, **7**, 15227.

4 J. Clarke, H. C. Wu, L. Jayasinghe, A. Patel, S. Reid and H. Bayley, *Nat. Nanotechnol.*, 2009, **4**, 265–270.

5 S. Mura, J. Nicolas and P. Couvreur, *Nat. Mater.*, 2013, **12**, 991–1003.

6 Y. R. Kim, S. Jung, H. Ryu, Y. E. Yoo, S. M. Kim and T. J. Jeon, *Sensors (Switzerland)*, 2012, **12**, 9530–9550.

7 J. R. Werber, C. O. Osuji and M. Elimelech, *Nat. Rev. Mater.*, 2016, **1**, 1–15.

8 A. G. Fane, R. Wang and M. X. Hu, *Angew. Chemie - Int. Ed.*, 2015, **54**, 3368–3386.

9 T. Ren, M. Erbakan, Y. Shen, E. Barbieri, P. Saboe, H. Feroz, H. Yan, S. McCuskey, J. F. Hall, a. B. Schantz, G. C. Bazan, P. J. Butler, M. Grzelakowski and M. Kumar, *Adv. Biosyst.*, 2017, **1**, 1700053.

10 Y. X. Shen, P. O. Saboe, I. T. Sines, M. Erbakan and M. Kumar, *J. Memb. Sci.*, 2014, **454**, 359–381.

11 C. G. Palivan, R. Goers, A. Najer, X. Zhang, A. Car and W. Meier, *Chem. Soc. Rev.*, 2016, **45**, 377–411.

12 S. W. Kowalczyk, T. R. Blosser and C. Dekker, *Trends Biotechnol.*, 2011, **29**, 607–614.

13 M. Garni, S. Thamboo, C. A. Schoenenberger and C. G. Palivan, *Biochim. Biophys. Acta - Biomembr.*, 2017, **1859**, 619–638.

14 W. K. Subczynski, J. S. Hyde and a Kusumi, *Proc. Natl. Acad. Sci.*, 1989, **86**, 4474–4478.

15 J. Gutknecht, *J. Gen. Physiol.*, 1988, **69**, 779–794.

16 A. Walter and J. Gutknecht, *J. Membr. Biol.*, 1986, **90**, 207–217.

17 E. Orbach and a Finkelstein, *J. Gen. Physiol.*, 1980, **75**, 427–436.

18 J. N. Yang and M. J. Hinner, *Methods Mol Biol.*, 2015, 29–57.

19 M. Freigassner, H. Pichler and A. Glieder, *Microb. Cell Fact.*, 2009, **8**, 1–22.

20 J. Kistler and R. M. Stroud, *Proc. Natl. Acad. Sci. U. S. A.*, 1981, **78**, 3678–82.

21 A. S. Verkman, Curr. Biol., 2013, **23**, 52-55.

22 H. Wang, T. S. Chung, Y. W. Tong, K. Jeyaseelan, A. Armugam, Z. Chen, M. Hong and W. Meier, *Small*, 2012, **8**, 1185–1190.

23 H. Wang, T. S. Chung, Y. W. Tong, W. Meier, Z. Chen, M. Hong, K. Jeyaseelan and A. Armugam, *Soft Matter*, 2011, **7**, 7274–7280.

24 H. X. Gan, H. Zhou, Q. Lin and Y. W. Tong, *Sci. Rep.*, 2017, **7**, 1–13.

25 X. Li, S. Chou, R. Wang, L. Shi, W. Fang, G. Chaitra, C. Y. Tang, J. Torres, X. Hu and A. G. Fane, *J. Memb. Sci.*, 2015, **494**, 68–77.

26 C. Y. Tang, Y. Zhao, R. Wang, C. Hélix-Nielsen and A. G. Fane, *Desalination*, 2013, **308**, 34–40.

27 P. H. H. Duong, T. S. Chung, K. Jeyaseelan, A. Armugam, Z. Chen, J. Yang and M. Hong, *J. Memb. Sci.*, 2012, **409-410**, 34–43.

28 G. Sun, T. S. Chung, K. Jeyaseelan and A. Armugam, *Colloids Surfaces B Biointerfaces*, 2013, **102**, 466–471.

29 H. L. Wang, T. S. Chung, Y. W. Tong, K. Jeyaseelan, A. Armugam, H. H. P. Duong, F. Fu, H. Seah, J. Yang and M. Hong, *J. Memb. Sci.*, 2013, **434**, 130–136.

30 W. Xie, F. He, B. Wang, T.-S. Chung, K. Jeyaseelan, A. Armugam and Y. W. Tong, *J. Mater. Chem. A*, 2013, **1**, 7592–7600.

31 D. Branton, D. W. Deamer, A. Marziali, H. Bayley, S. A. Benner, T. Butler, M. Di Ventra, S. Garaj, A. Hibbs, X. Huang, S. B. Jovanovich, P. S. Krstic, S. Lindsay, X. S. Ling, C. H. Mastrangelo, A. Meller, J. S. Oliver, Y. V. Pershin, J. M. Ramsey, R. Riehn, G. V. Soni, V. Tabard-Cossa, M. Wanunu, M. Wiggin and J. A. Schloss, *Nat. Biotechnol.*, 2008, **26**, 1146–1153.

32 O. Braha, B. Walker, S. Cheley, J. J. Kasianowicz, L. Song, J. E. Gouaux and H. Bayley, *Chem. Biol.*, 1997, **4**, 497–505.

33 X. F. Kang, L. Q. Gu, S. Cheley and H. Bayley, *Angew. Chemie - Int. Ed.*, 2005, **44**, 1495–1499.

34 A. Meller, L. Nivon, E. Brandin, J. Golovchenko and D. Branton, *PNAS*, 2000, **97**, 1079-1084.

35 X. Zhang, W. Fu, C. G. Palivan and W. Meier, *Sci. Rep.*, 2013, **3**, 2196.

36 D. W. Urry, M. C. Goodall, J. D. Glickson and D. F. Mayers, *Proc. Natl. Acad. Sci. U. S. A.*, 1971, **68**, 1907–1911.

37 J. R. Elliott, D. Needham, J. P. Dilger and D. A. Haydon, *BBA - Biomembr.*, 1983, **735**, 95–103.

38 D. A. Kelkar and A. Chattopadhyay, *Biochim. Biophys. Acta - Biomembr.*, 2007, **1768**, 2011–2025.

39 R. Koebnik, K. P. Locher and P. Van Gelder, *Mol. Microbiol.*, 2000, **37**, 239–253.

40 D. E. Discher and A. Eisenberg, *Science (80-.).*, 2002, **297**, 967–973.

41 H. Hauser, M. C. Phillips and M. Stubbs, Nature, 1972, **239**, 342-344.

42 H. Bermudez, A. K. Brannan, D. a. Hammer, F. S. Bates and D. E. Discher, *Macromolecules*, 2002, **35**, 8203–8208.

43 C. Nardin, M. Winterhalter and W. Meier, *Langmuir*, 2000, **16**, 7708–7712.

44 B. M. Discher, Y. Y. Won, D. S. Ege, J. C. M. Lee, F. S. Bates, D. E. Discher and D. A. Hammer, *Science (80-.).*, 1999, **284**, 1143–1146.

45 J. Kowal, X. Zhang, I. A. Dinu, C. G. Palivan and W. Meier, *ACS Macro Lett.*, 2014, **3**, 59–63.

46 E. Kaditi, G. Mountrichas and S. Pispas, *Eur. Polym. J.*, 2011, **47**, 415–434.

47 A. Gress, B. Smarsly and H. Schlaad, *Macromol. Rapid Commun.*, 2008, **29**, 304–308.

48 M. Obeng, A. H. Milani, M. S. Musa, Z. Cui, L. A. Fielding, L. Farrand, M. Goulding and B. R. Saunders, *Soft Matter*, 2017, **13**, 2228–2238.

49 Z.-C. Li, Y.-Z. Liang, G.-Q. Chen and F.-M. Li, *Macromol. Rapid Commun.*, 2000, **21**, 375–380.

50 C.-Y. Yu, S.-H. Wen, S.-H. Yu and C.-C. Wang, *J. Polym. Sci. Part A Polym. Chem.*, 2018, **56**, 67–74.

51 X.-B. Xiong, Z. Binkhathlan, O. Molavi and A. Lavasanifar, *Acta Biomater.*, 2012, **8**, 2017–2033.

52 M. van Dijk, D. T. S. Rijkers, R. M. J. Liskamp, C. F. van Nostrum and W. E. Hennink, *Bioconjug. Chem.*, 2009, **20**, 2001–2016.

53 P. V. Pawar, S. V. Gohil, J. P. Jain and N. Kumar, *Polym. Chem.*, 2013, **4**, 3160–3176.

54 M.-H. Li and P. Keller, *Soft Matter*, 2009, **5**, 927–937.

55 F. Schacher, M. Ulbricht and A. H. E. Müller, *Adv. Funct. Mater.*, 2009, **19**, 1040–1045.

56 S. Li, F. Meng, Z. Wang, Y. Zhong, M. Zheng, H. Liu and Z. Zhong, *Eur. J. Pharm. Biopharm.*, 2012, **82**, 103–111.

57 C. Nardin, T. Hirt, J. Leukel and W. Meier, *Langmuir*, 2000, **16**, 1035–1041.

58 M. Grzelakowski, O. Onaca, P. Rigler, M. Kumar and W. Meier, *Small*, 2009, **5**, 2545–2548.

59 M. Winterhalter, *Curr. Opin. Colloid Interface Sci.*, 2000, **5**, 250–255.

60 C. Nardin, M. Winterhalter and W. Meier, *Angew Chemie*, 2000, **39**, 4599–4602.

61 D. Wong, T. J. Jeon and J. Schmidt, *Nanotechnology*, 2006, **17**, 3710–3717.

62 D. Ho, S. Chang and C. D. Montemagno, *Nanomedicine Nanotechnology, Biol. Med.*, 2006, **2**, 103–112.

63 S. Belegrinou, J. Dorn, M. Kreiter, K. Kita-Tokarczyk, E.-K. Sinner and W. Meier, *Soft Matter*, 2010, **6**, 179–186.

64 S. Edmondson, V. L. Osborne and W. T. S. Huck, *Chem. Soc. Rev.*, 2004, **33**, 14–22.

65 J. Dorn, S. Belegrinou, M. Kreiter, E. K. Sinner and W. Meier, *Macromol. Biosci.*, 2011, **11**, 514–525.

66 R. A. Dixon and I. Chopra, *J. Antimicrob. Chemother.*, 1986, **18**, 557–563.

67 J. T. Kowal, J. K. Kowal, D. Wu, H. Stahlberg, C. G. Palivan and W. P. Meier, *Biomaterials*, 2014, **35**, 7286-7294.

68 A. González-Pérez, K. B. Stibius, T. Vissing, C. H. Nielsen and O. G. Mouritsen, *Langmuir*, 2009, **25**, 10447–10450.

69 P. S. Zhong, T. S. Chung, K. Jeyaseelan and A. Armugam, *J. Memb. Sci*., 2012, **407-408**, 27-33.

70 P. Vermette, L. Meagher, E. Gagnon, H. J. Griesser and C. J. Doillon, *J. Control. Release*, 2002, **80**, 179–195.

71 D. Stamou, C. Duschl, E. Delamarche and H. Vogel, *Angew. Chemie - Int. Ed.*, 2003, **42**, 5580–5583.

72 X. Zhang, M. Lomora, T. Einfalt, W. Meier, N. Klein, D. Schneider and C. G. Palivan, *Biomaterials*, 2016, **89**, 79–88.

73 S. Balme, J. M. Janot, L. Berardo, F. Henn, D. Bonhenry, S. Kraszewski, F. Picaud and C. Ramseyer, *Nano Lett.*, 2011, **11**, 712–716.

74 S. Wu, S. R. Park and X. S. Ling, *Nano Lett.*, 2006, **6**, 2571–2576.

75 S. Balme, F. Picaud, S. Kraszewski, P. Déjardin, J. M. Janot, M. Lepoitevin, J. Capomanes, C. Ramseyer and F. Henn, *Nanoscale*, 2013, **5**, 3961–3968.

76 A. Abou Chaaya, M. Le Poitevin, S. Cabello-Aguilar, S. Balme, M. Bechelany, S. Kraszewski, F. Picaud, J. Cambedouzou, E. Balanzat, J. M. Janot, T. Thami, P. Miele and P. Dejardin, *J. Phys. Chem. C*, 2013, **117**, 15306–15315.

77 G. Roussel, A. Matagne, X. De Bolle, E. A. Perpète and C. Michaux, *Protein Expr. Purif.*, 2012, **83**, 198–204.

78 G. Roussel, E. A. Perpète, A. Matagne, E. Tinti and C. Michaux, *Biotechnol. Bioeng.*, 2013, **110**, 417–423.

79 M. Lopes-Rodrigues, J. Triguero, J. Torras, E. A. Perpète, C. Michaux, D. Zanuy and C. Alemán, *Biophys. Chem.*, 2018, **234**, 6–15.

80 M. M. Pérez-Madrigal, L. J. del Valle, E. Armelin, C. Michaux, G. Roussel, E. A. Perpète and C. Alemán, *ACS Appl. Mater. Interfaces*, 2015, **7**, 1632–1643.

81 A. Puiggalí-Jou, M. M. Pérez-Madrigal, L. J. del Valle, E. Armelin, M. T. Casas, C. Michaux, E. A. Perpète, F. Estrany and C. Alemán, *Nanoscale*, 2016, **8**, 16922–16935.

82 A. Puiggali-Jou, J. Medina, L. J. Del Valle and C. Alemn, *Eur. Polym. J.*, 2016, **75**, 552–564.

83 M. Lopes-Rodrigues, A. Puiggalí-Jou, D. Martí-Balleste, L. J. Del Valle, C. Michaux, E. A. Perpète and C. Alemán, *ACS Omega*, 2018, **3**, 7856–7867.

84 A. Puiggalí-jou, J. Pawlowski, L. J. Valle, E. A. Perpète, S. Sek and C. Alemán, *ACS Omega*, 2018, **3**, 9003–9019.

85 J. R. Werber and M. Elimelech, *Sci. Adv.*, 2018, **4**, 1–10.

86 J. R. Werber, C. J. Porter and M. Elimelech, *Environ. Sci. Technol.*, 2018, **52**, 10737–10747.

87 P. O. Saboe, E. Conte, S. Chan, H. Feroz, B. Ferlez, M. Farell, M. F. Poyton, I. T. Sines, H. Yan, G. C. Bazan, J. Golbeck and M. Kumar, *J. Mater. Chem. A*, 2016, **4**, 15457–15463.

88 M. Tanaka and E. Sackmann, *Nature*, 2005, **437**, 656-663.

89 A. A. Brian and H. M. McConnell, *Proc. Natl. Acad. Sci. U. S. A.*, 1984, **81**, 6159–6163.

90 E. M. Erb, K. Tangemann, B. Bohrmann, B. Muller and J. Engel, *Biochem.*, 1997, **36**, 7395–7402.

91 A. Kloboucek, A. Behrisch, J. Faix and E. Sackmann, *Biophys. J.*, 1999, **77**, 2311–2328.

92 S. Y. Qi, J. T. Groves and A. K. Chakraborty, *Proc. Natl. Acad. Sci.*, 2001, **98**, 6548–6553.

93 A. Grakoui, S. K. Bromley, C. Sumen, M. M. Davis, A. S. Shaw, P. M. Allen and M. L. Dustin, *Science*, 1999, **285**, 221–227.

94 L. K. Tamm and H. M. McConnell, *Biophys. J.*, 1985, **47**, 105–113.

95 P. Y. Chan, M. B. Lawrence, M. L. Dustin, L. M. Ferguson, D. E. Golan and T. A. Springer, *J. Cell Biol.*, 1991, **115**, 245–255.

96 E. K. Sinner and W. Knoll, *Curr. Opin. Chem. Biol.*, 2001, **5**, 705–711.

97 N. Sakai and S. Matile, *Langmuir*, 2013, **29**, 9031–9040.

98 S. Matile, A. Vargas Jentzsch, J. Montenegro and A. Fin, *Chem. Soc. Rev.*, 2011, **40**, 2453–2474.

99 C. Ren, X. Ding, A. Roy, J. Shen, S. Zhou, F. Chen, S. F. Yau Li, H. Ren, Y. Y. Yang and H. Zeng, *Chem. Sci.*, 2018, **9**, 4044–4051.

100 C. Lang, X. Deng, F. Yang, B. Yang, W. Wang, S. Qi, X. Zhang, C. Zhang, Z. Dong and J. Liu, *Angew. Chemie - Int. Ed.*, 2017, **56**, 12668–12671.

101 T. Muraoka, K. Umetsu, K. V. Tabata, T. Hamada, H. Noji, T. Yamashita and K. Kinbara, *J. Am. Chem. Soc.*, 2017, **139**, 18016–18023.

CAPTIONS TO FIGURES

Figure 1. (a) Membrane topography of the Aq monomer (left) and crystal structure (side view, left; top view, right) with four water molcules (red balls) shown in aqueous pore region. Helices are labelled H1–H8. Reproduced with permission from reference 21. (b) Strand-sequencing using ionic current blockage. A typical trace of the ionic current amplitude (left) through an α-HL pore clearly differentiates between an open pore (top right) and one blocked by a strand of DNA (bottom right) but cannot distinguish between the ~12 nucleotides that simultaneously block the narrow transmembrane channel domain (red bracket). Reproduced with permission from reference 31. (c) Top view of the gA channel as a space-filling model (color code: white, carbon atoms; blue, nitrogen atoms; red, oxygen atoms) using coordinates from PDB 1MAG. Note how the alternating L–D arrangement allows all amino acid side chains to project outward from the channel lumen and the channel lumen is lined by the peptide backbone. (d) Axial and equatorial views of crystallized OmpF, a representative MP. Reproduced with permission from reference 79.

Figure 2. Lipoic acid (LA)-functionalized PB-PEO vesicles spread onto a bare gold surface**.** Reproduced with permission from reference 65. (b) PB-PEO-OH and PB-PEO-LA were transferred onto gold substrates by applying consecutively the Langmuir-Blodgett (LB) and Langmuir-Schaefer (LS) techniques to form a polymer tethered bilayer (left), where the protein was inserted (right). Reproduced with permission from reference 35.

Figure 3. (a) Representation of MP insertion when using Bio-Beads (BB) into solid-supported polymer membrane. (b) Conductance measured when a voltage of 40 mV is applied on bare Au, the bilayer, the bilayer with the protein incorporated using Bio-Beads (bilayer+MloK1+BB), the bilayer with the protein (bilayer+MloK1), and the

bilayer with the Bio-Beads (bilayer+BB). Reproduced with permission from reference 67.

Figure 4. Schematic illustration of pore-spanning membrane on the PCTE: design and synthesis. (a) Incorporation of AqpZ in PMOXA−PDMS−PMOXA (ABA copolymer) vesicles. (b) Surface modification of the PCTE membrane support in a two-step process: (i) coating with a monolayer of cysteamine through chemisorption; and (ii) the primary amine are converted to acrylate residues via conjugating with acrylic acid. (c) Pressure-assisted vesicle adsorption on the PCTE support. (d) Covalent-conjugation-driven vesicle rupture and pore-spanning membrane formation. Reproduced with permission from reference 22.

Figure 5. Field-emission scanning electron microscopy (a-c) and atomic force microscopy images (d-f) of the gold coated alumina substrate (a and d), the substrate covered with the polymer membrane (b and e), and the substrate covered with the AqpZ-incorporated polymer membrane (c and f). Reproduced with permission from reference 27.

Figure 6. Field-emission scanning electron microscopy of (a) CA, (b) silanized CA, and (c) AqpZ-containing PMOXA−PDMS−PMOXA triblock copolymer. Reproduced with permission from reference 69.

Figure 7. Schemes of AqpZ-embedded vesicular membrane at the top: (a) AqpZ reconstitution into the vesicles formed from ABA block copolymer blends. DDM stands for dodecyl-b-D-maltoside, a detergent for protein stabilization; (b) Immobilization of the vesicles onto the substrate by pressure; (c) addition of the self-assembled monolayer of cysteamine; and (d) PDA-His coating on the top of the membrane. (e-h) Field-emission scanning electron microscopy micrographs at the bottom: (e) gold-coated PCTE membrane with a self-assembled monolayer of cysteamine (pore size 50 nm); (f)

PCTE membrane with 3-cycle coating of PDA–His on the top of chemisorbed cysteamine (control); and (g) vesicles immobilized on the PCTE membrane with 3-cycle coating of PDA–His on top. The micrograph displayed in (h) corresponds to a zoom of (g). Adapted with permission from reference 29.

Figure 8. (a) Schematic diagram of the Aqpz-vesicle imprinted membrane preparation: (1) Aqpz-polymer vesicles, (2) porous CA membrane substrate, (3) Aqpz vesicles immobilized on the porous membrane, (4) Aqpz-vesicle-imprinted membrane, and (5) cross-section of the Aqpz-vesicle-imprinted membrane. (b-g) Field-emission scanning electron microscopy micrographs displayed the membrane morphologies: (b, c) top surface and cross-section of the porous substrate CA membrane; (d, e) non-vesicle-imprinted membrane; and (f, g) Aqpz-vesicle-imprinted membrane. Adapted with permission from reference 30.

Figure 9: (a) GlpF molecular representation (green) together with ribitol, as a model sugar alcohol (red). Side (right) and front (left) views are represented. (b) Schematic representation of a functionalized surface serving as a sugar alcohol biosensor based on immobilized proteopolymersome nanoreactors with selective transport due to the GlpF presence and detection of sugar alcohols due to the encapsulated enzymes. Adapted with permission from reference 72.

Figure 10. Procedure scheme for the fabrication of nanoperforated membranes, the modification of nanopore size by atomic layer deposition (ALD), the creation of hydrophobic pore surfaces by vapour exposure treatment with hexamethyldisilazane (HMDS), and the immobilization of gA. Adapted with permission from reference 76.

Figure 11. Surface morphology of (a) PNMPy−Omp2a, (b) PNMPy and (c) nanoperforated PLA membranes: low- and high-magnification SEM micrographs are displayed at the left and the right, respectively. Adapted with permission from

references 80 and 81. (d) 3D AFM phase images of the skin surfaces of nanoperforated PLA nanomembranes before (left) and after (right) incubation with a 0.5 mg/mL Omp2a solution. Adapted with permission from reference 81.

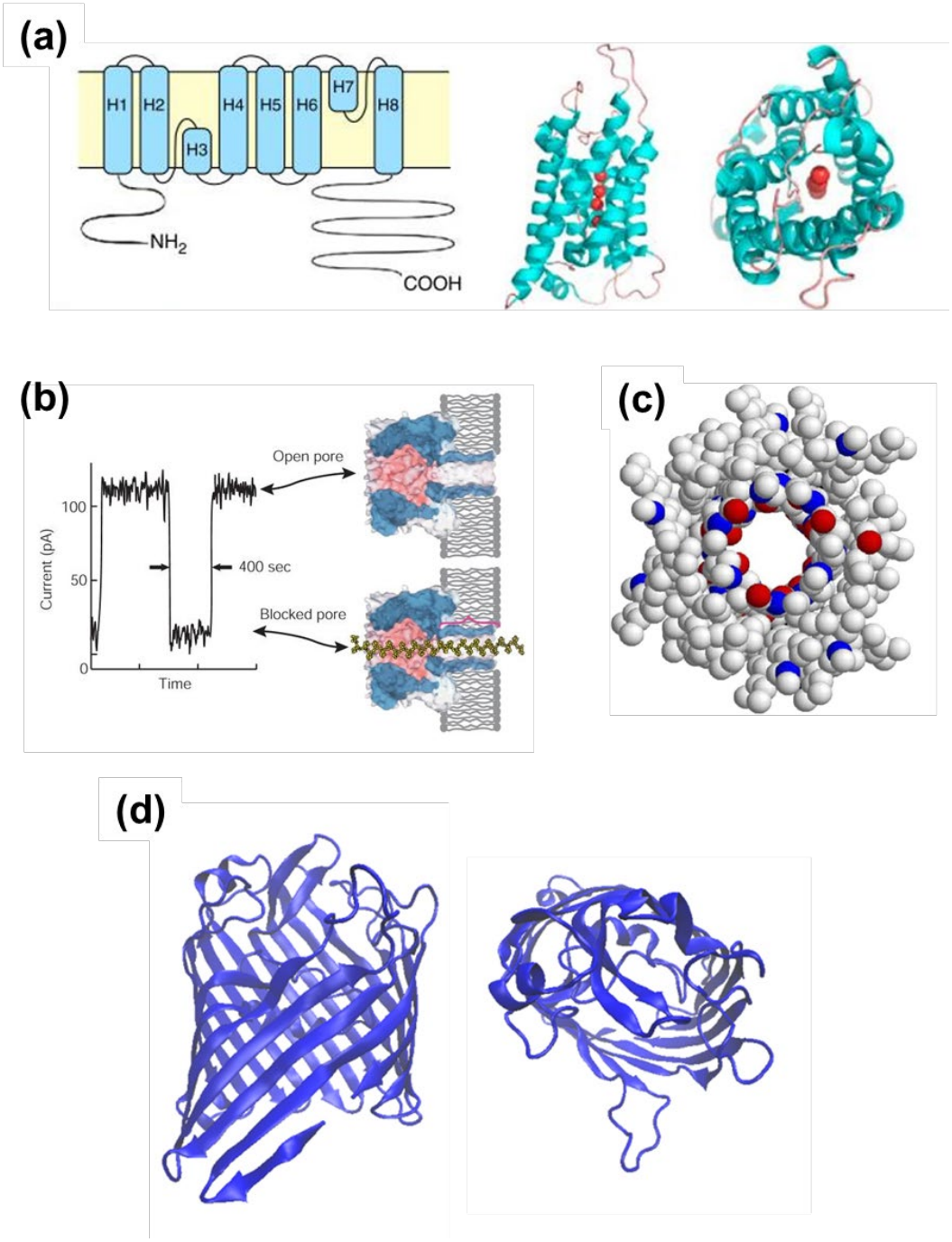
(a)
H1
H2
H3
H4
H5
H6
H7
H8
NH2
COOH
(b)
Open pore
Blocked pore
400 sec
Current (pA)
100
50
0
Time
(c)
(d)

Figure 1

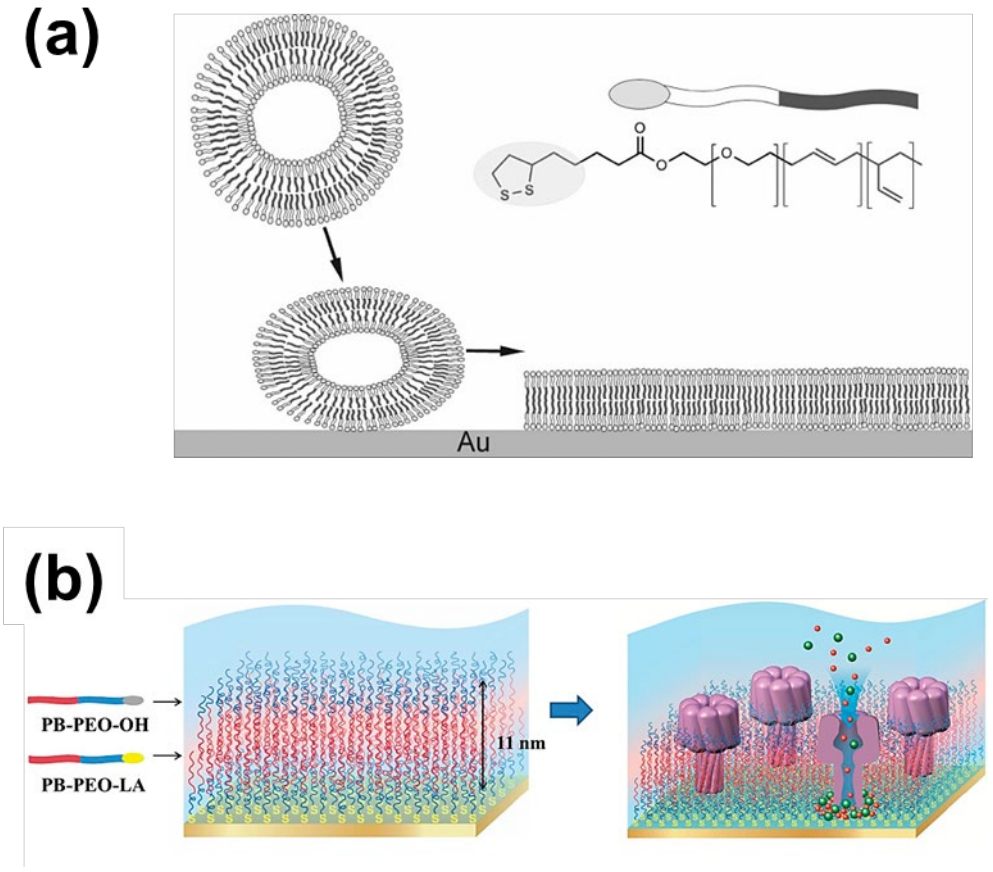

Figure 2

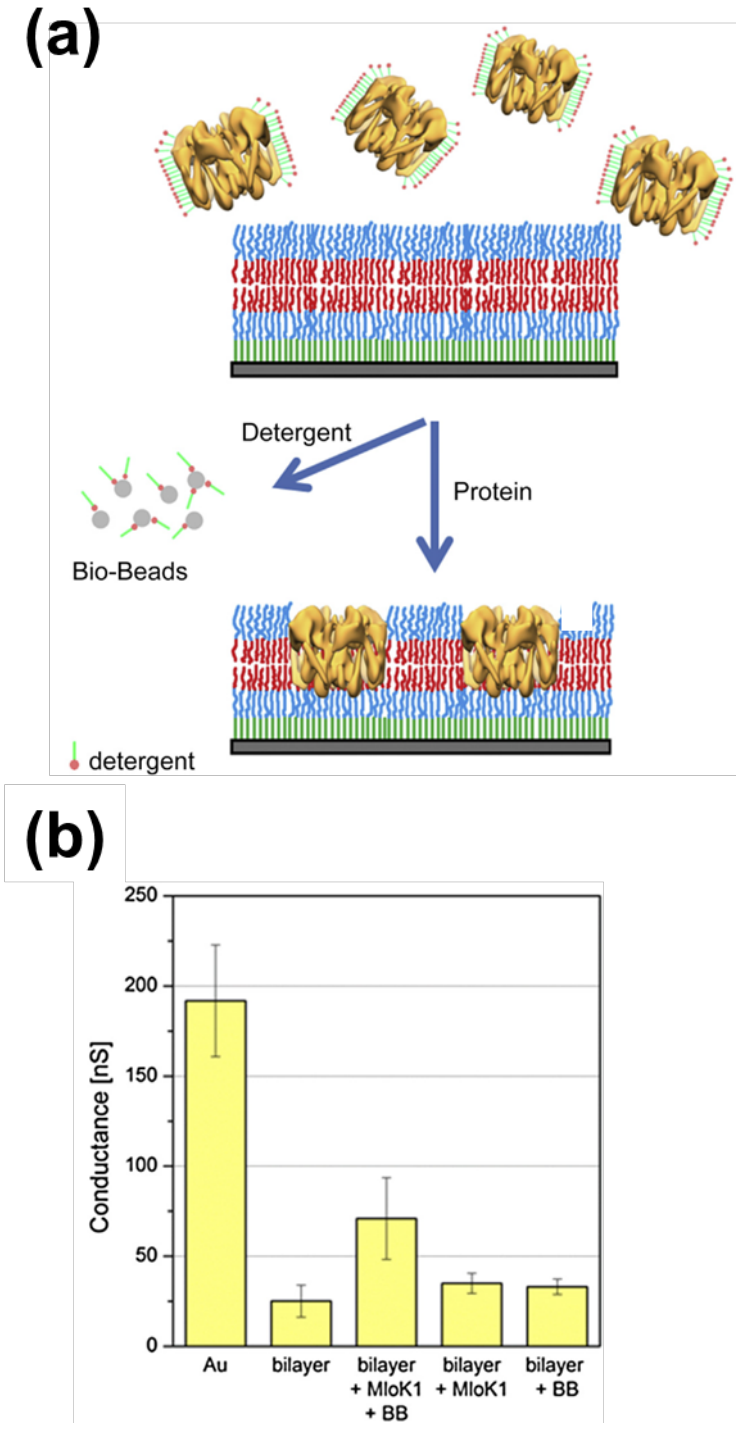
(a)
Detergent
Protein
Bio-Beads
detergent
(b)
Conductance [nS]
250
200
150
100
50
0
Au
bilayer
bilayer + MloK1 + BB
bilayer + MloK1
bilayer + BB

Figure 3

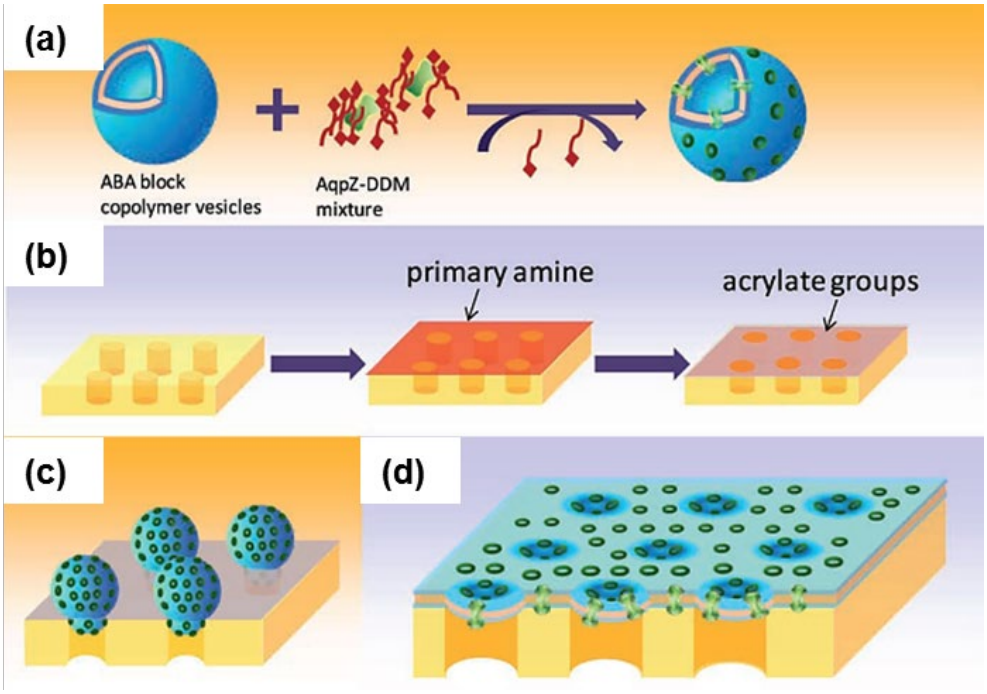
(a)
ABA block
copolymer vesicles
AqpZ-DDM
mixture
(b)
primary amine
acrylate groups
(c)
(d)

Figure 4

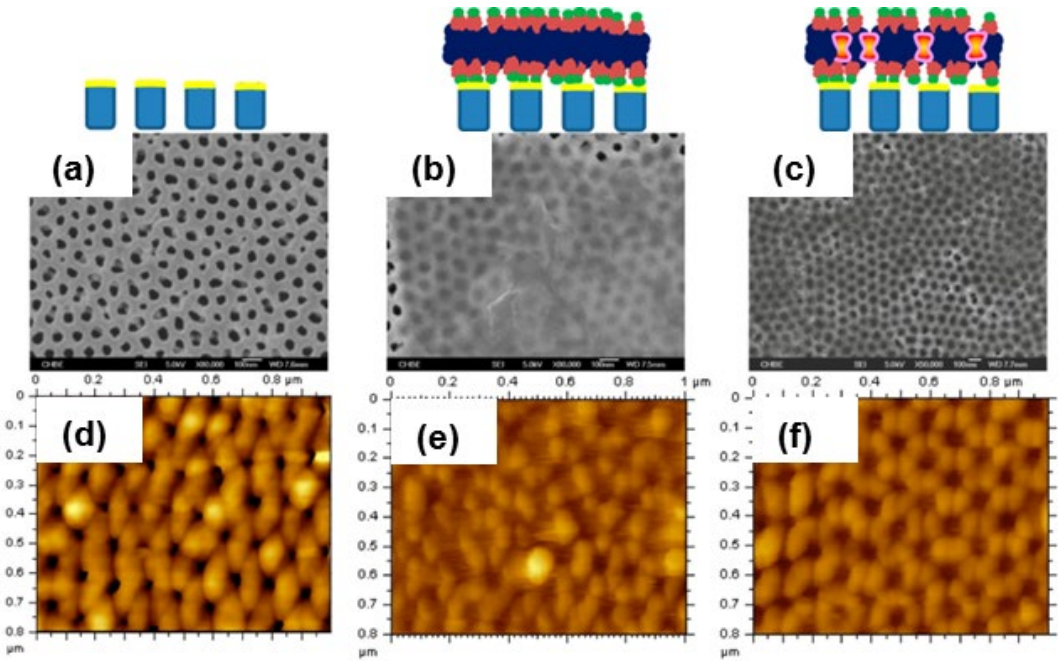

Figure 5

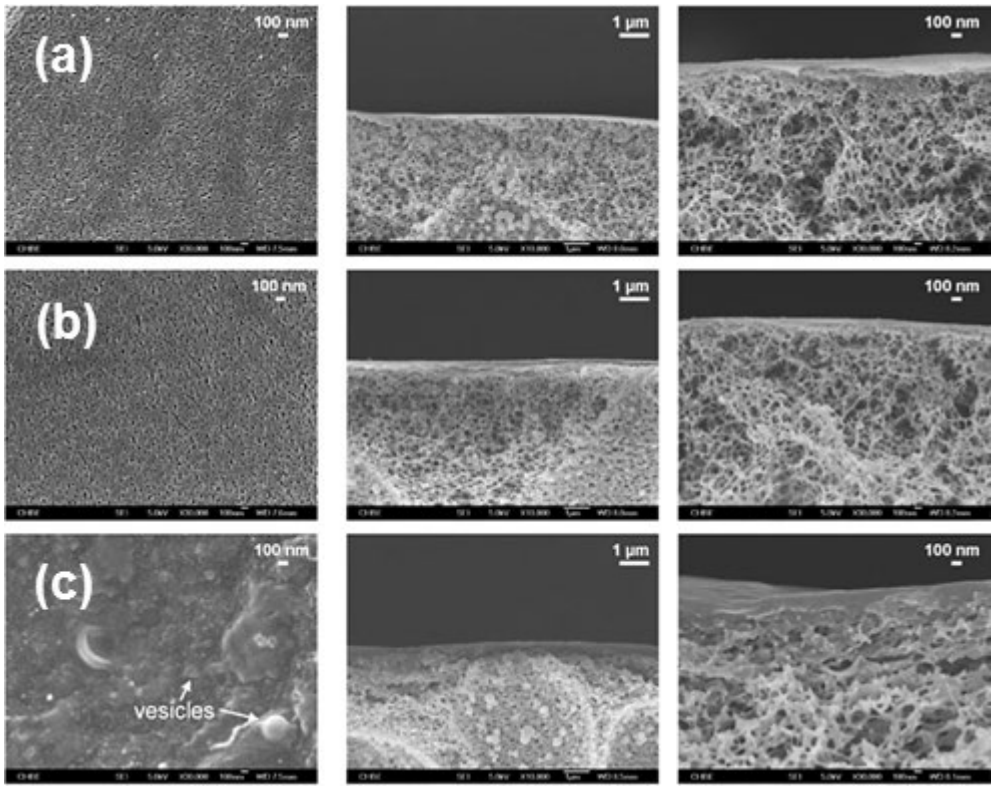
(a)
100 nm
1 μm
100 nm
(b)
100 nm
1 μm
100 nm
(c)
100 nm
vesicles
1 μm
100 nm

Figure 6

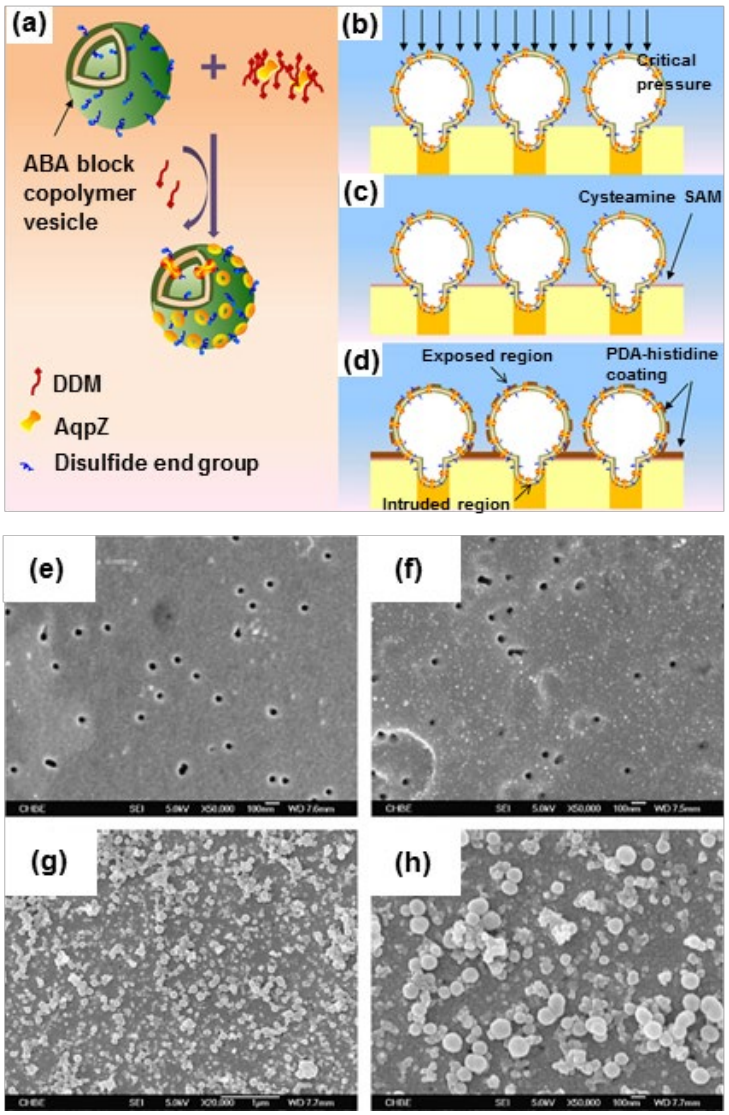
(a)
ABA block copolymer vesicle
DDM
AqpZ
Disulfide end group
(b)
Critical pressure
(c)
Cysteamine SAM
(d)
Exposed region
PDA-histidine coating
Intruded region
(e)
(f)
(g)
(h)

Figure 7

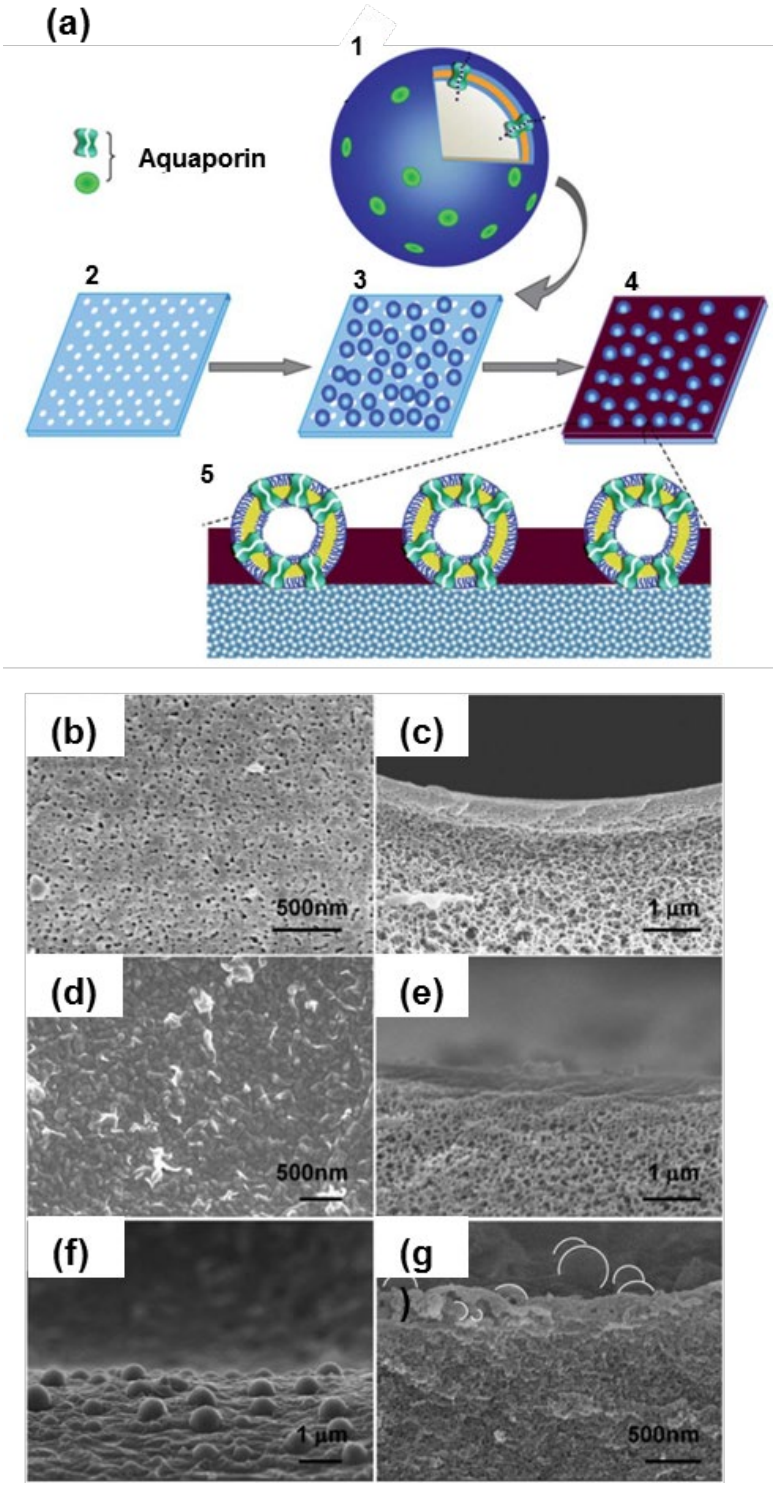

Figure 8

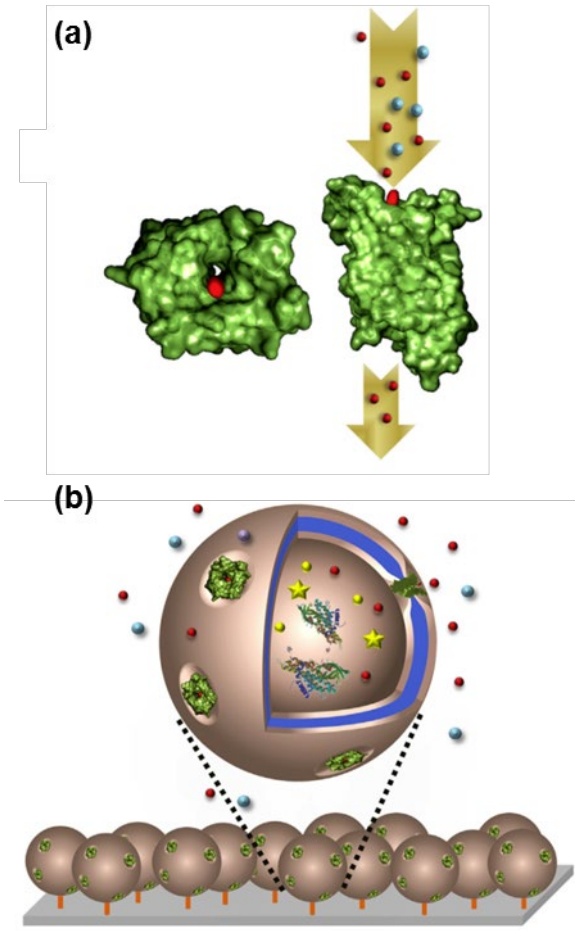

Figure 9

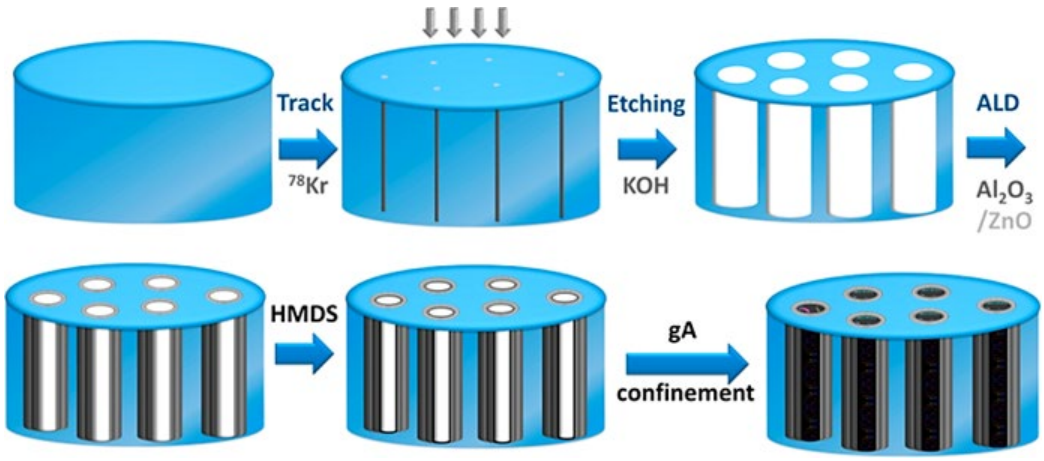

Figure 10

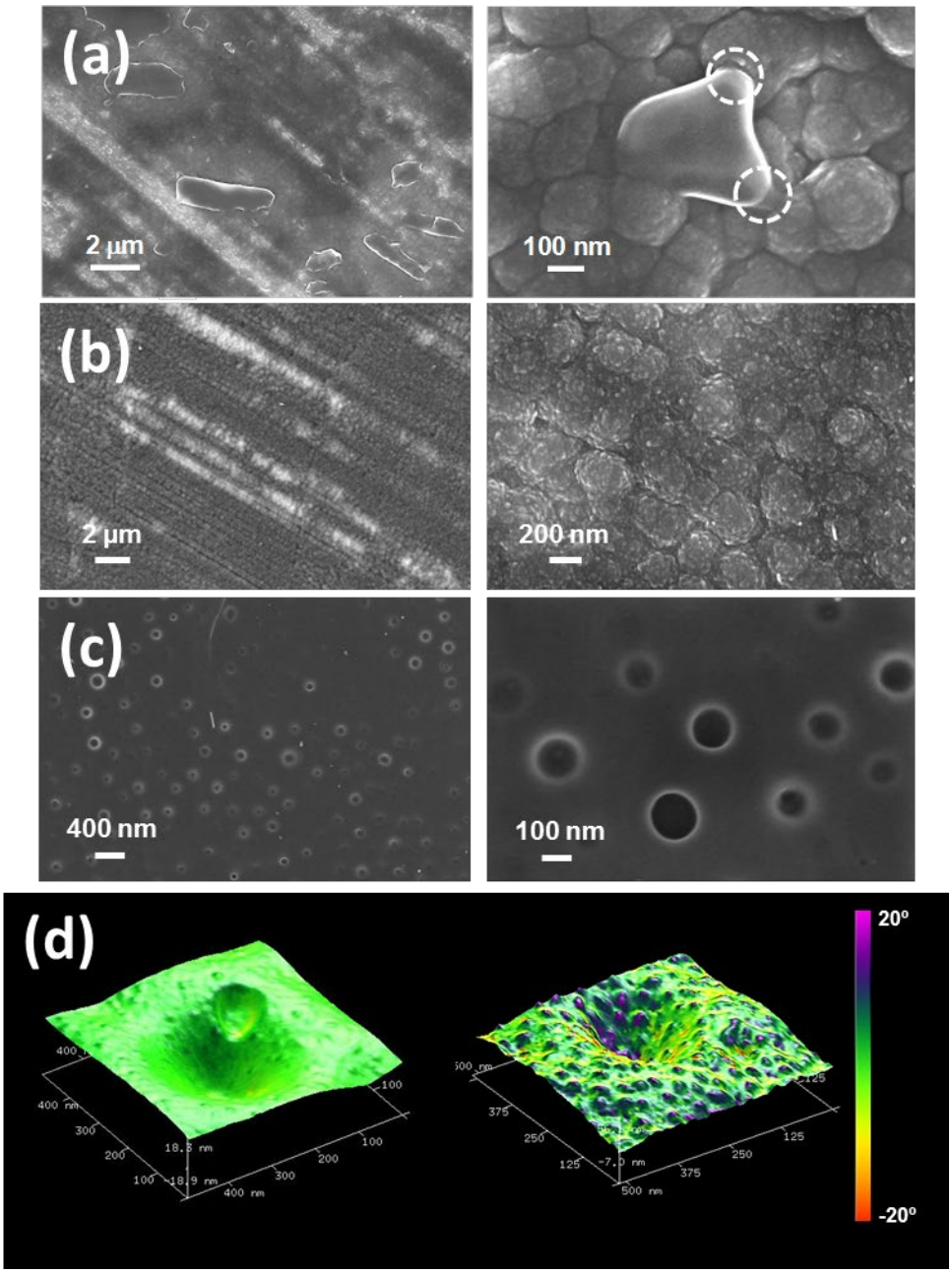

Figure 11

Table 1. Summary of the most important characteristics (*i.e.* preparation method, polymer, protein and activity) of biomimetic membranes made of polymers.

Type	Support	Polymer	Protein	Functionality	Permeability	Ref.
Free-standing	-	PMOXA-*b*-PDMS-*b*-PMOXA	OmpF and maltoporin	Electrophysiological studies	σ increment of 6 nS (OmpF) and 4 nS (maltoporin)	60
	-	PMOXA-*b*-PDMS-*b*-PMOXA	OmpG and Alamethicin	Electrophysiological studies	σ= 0.72 ± 0.06 nS (OmpG) and σ= 0.3, 1.1, 2.22 and 3.34 nS (alamethicin)	61
	Air-water interface	PMOXA-*b*-PDMS-*b*-PMOXA	OmpF	Mechanical studies	Shorter copolymer chains possess enhanced biomimicry of natural lipid-based membranes	62
Solid supported	Au	PB-PEO-OH and PB-PEO-LA	Polymyxin B	Peptide effect on membrane resistance	Reduction of the resistance from 4.4 to 1.2 $M\Omega \cdot cm^2$	66
	SiO_2 wafers, glass and Au	PDMS-*b*-PMOXA with amino-linker	MloK1	Ion flow	σ= 39.5 ± 7.5 nS	67
	Au	Functionalized PB-PEO	αHL	Ion flow	σ= 31 ns	35
Porous solid support-polym	PCTE	PMOXA-PDMS -PMOXA	AqpZ	Water purification	Maximum water flux 16.4 ± 1.5L m^{-2} h^{-1} (LMH) with a salt rejection of	22

					98.8%	
	Commercially available CA with pores	PMOXA-*b*-PDMS-PMOXA	AqpZ	Water purification	Maximum water flux 34.19 ± 6.90 LMH/bar with a 200 ppm NaCl salt rejection of 32.86 ± 9.12%	69
	Porous alumina	functionalized PMOXA-PDMS-PMOXA	AqpZ	Water nanofiltration	Maximum water flux 8 LMH/bar with a salt rejection of 45.1 ± 4.2%	27
	Tefzel ethylene tetrafluoroethylene(ETFE)	PMOXA-*b*-PDMS-*b*-PMOXA	gA	Electrophysiological studies	gA is inserted and is functional	68
Porous solid support-polymersome intrusion	Au-coated PCTE	PMOXA-PDMS-PMOXA functionalized with end groups	AqpZ	Seawater desalination and water reuse	Water flux 17.6 LMH with high salt rejection 91.8%	29
	CA membrane with pore size of ~25 nm and functionalized surface	PMOXA-PDMS-PMOXA	AqpZ	Nanofiltration or forward osmosis	5.58 ± 0.97 LMH with a salt rejection of 50.7%	30
Immobilized polymersome	Glass surfaces chemically modified with amino groups	PMOXA-*b*-PDMS-*b*-PMOXA	GlpF	Selective detection of sugar alcohols	The lowest concentration of ribitol detected was 200 nM	72
	Glass slide with BSA-biotin-streptavidin-biotin-nanoreactor link	PMOXA-*b*-PDMS-*b*-PMOXA	OmpF	Nanoreactors for studying model enzymatic reactions	The K_m of the enzyme entrapped on the immobilized polymersome was 46mM.	58

Protein confinement in porous insulating polymer	PET film tuned by atomic layer deposition of Al2O3/ZnO	PET	gA	Study of protein selectivity to ions	Conductance is one order of magnitude bigger when gA is inserted. Cl^- permeability is higher than Na^+	76
	Free-standing	PCTE covered with PVP	gA	Study of protein selectivity to ions	No significant ion selectivity is observed between the mono and divalent cations	73
	Free-standing	PCTE covered with PVP and treated with ethanol	gA	Study of protein selectivity to ions	Enhanced conductivity of K^+ *vs* Na^+	75
	Free-standing / ITO	PLA with nanoperforations	Omp2a	Study of protein selectivity to ions	Enhanced conductivity of K^+ *vs* Na^+	81
Solid membrane conducting polymer	CP film supported onto steel	PPy	Omp2a	Study of protein selectivity to ions	Enhanced conductivity of K^+ *vs* Na^+	80

Table 2. Summary of the advantages and disadvantages encountered during the preparation and application of the different type of biomimetic membranes made of polymers.

Technique	Sub-technique	Advantages	Disadvantages	Ref.
Amphiphilic polymers/Block copolymers	Free standing	No influence of the substrate. Direct measure.	Low stability. No more than 1 mm^2 in area. Difficult scalability to support industrial applications	60-62
	Solid supported	Increased stability. Easy to measure the influence of the protein if the substrate is a conductive material.	Interactions with the substrate can induce the denaturation of the protein. Poor area coverage. Membrane defects. Difficult scalability to support industrial applications	35,65,67
	Porous solid support-polymersome spanning	The protein is not in direct contact with the substrate. There is more than enough space for the solutes to cross the membrane.	The porous substrate normally needs a pre-treatment to facilitate proteopolymersome spanning. Poor area coverage. Membrane defects. Difficult scalability to support industrial applications.	22,27,69,68
	Porous solid support-polymersome intrusion	Easier to cover all the perforations. The protein is not in direct contact with the substrate. The final material is more selective and sensible since the electrolyte needs to cross two times the membrane.	Difficult scalability to support industrial applications.	29,30

	Polymersomes covalently linked to the surface	The proteopolymersomes are covalently linked to the substrate, providing stability.	Indirect measurement. Need to encapsulate enzymes inside the proteopolymersomes.	58,72
Nanostructured solid-state membrane	Insulating polymers	The scalability is higher. There are commercial membranes that can be used. The stability is higher and can be employed for actual applications.	Fine tune on the pore size realized on the membrane is needed. Difficult to control the correct deposition of the membrane protein on the pore.	73,75,76,81
	Conducting polymers	The polymerization can take place at the same time that the protein is embedded applying low voltages.	Influence of the polymer on the electrical measurements. High roughness and thickness which difficult the protein localization on the membrane. Difficult scalability to support industrial applications.	80

Graphical Abstract